Journal of Crystal Growth 311 (2009) 495–499

Contents lists available at ScienceDirect

Journal of Crystal Growth

journal homepage: www.elsevier.com/locate/jcrysgro

Synthesis and field emission properties of triangular-shaped GaN nanowires on Si(1 0 0) substrates

Duc V. Dinh [a], S.M. Kang [b], J.H. Yang [a], S.-W. Kim [c], D.H. Yoon [a,b,*]

[a] SKKU Advanced Institute of Nanotechnology (SAINT), Sungkyunkwan University, Suwon 440-746, Republic of Korea
[b] School of Advanced Materials Science & Engineering, Sungkyunkwan University, Suwon 440-746, Republic of Korea
[c] School of Advanced Materials and System Engineering, Kumoh National Institute of Technology, Gumi, Gyeongbuk 730–701, Republic of Korea

ARTICLE INFO

Available online 21 September 2008

PACS:
81.10.Bk
81.07.−b
81.05.Ea
85.45.Db

Keywords:
A1. Nanostructures
A3. Vapor-phase epitaxy
B1. Nitrides
B2. Semiconducting gallium compounds

ABSTRACT

Gallium nitride (GaN) nanowires, grown on gold-coated n-type Si(1 0 0) substrates, were synthesized using the vapor-phase epitaxy method. The grown GaN nanowires, with diameters in the range 20–60 nm and lengths of several micrometers, were uniformly distributed on Si substrates. The GaN nanowires were grown via a vapor–liquid–solid mechanism. The characteristics of the grown GaN were investigated using X-ray diffraction, micro-Raman, and transmission electron microscopy, which found that the GaN nanowires on the Si(1 0 0) are of good crystalline quality. The electron field emission properties of the GaN nanowires (at room temperature) showed a low turn-on field of ~3.96 V/μm and a field enhancement factor of ~1050. The sharp ends and rough surfaces of the GaN nanowires are responsible for their good field emission properties.

1. Introduction

One-dimensional (1D) nanostructures, such as nanotubes, nanobelts, nanorods, and nanowires, having wide applications in nano-electronics and nano-photonics as potential ideal building blocks for nano-scale electronics and mechanical devices, have been broadly researched [1–3]. Due to the high aspect ratios of 1D nanostructures, one of their most important uses is as electron field emission (FE) sources. Interestingly, the geometries of the 1D nanostructures strongly affect the FE properties and turn-on field [4].

Gallium nitride (GaN) is a semiconducting material that has a direct wide band gap of 3.39 eV at room temperature (RT). Compared to single-walled carbon nanotubes and ZnO nanowires, whose work functions are about 4.9 and 5.3 eV, respectively [5,6], GaN has a lower work function of 4.1 eV, stronger thermal stability, mechanical hardness, chemical stability, and a lower electron affinity of 2.7–3.3 eV [7]. Therefore, GaN cold cathodes probably obtain high electron emission current densities and low operation voltages. For these reasons, GaN may be a promising material for field emitters for optoelectronic device applications, such as laser diodes, light-emitting diodes, and high-power electronic device applications [8]. Previous studies on the FE properties of 1D GaN nanostructures focused on morphologies such as nanobelts [9], prismatic rods and cone nanowires [10], needle-like nanowires [11], and nanowires [12–14]. However, there have been no reports regarding the FE properties of triangular-shaped GaN nanowires grown via vapor-phase epitaxy (VPE). For FE characteristics of GaN nanostructures, Si(1 0 0) substrates are commonly used because of well-characterized electrical properties, good compatibility for integrated circuit technology, and optoelectronic device applications.

In this study, we synthesized high-quality triangular-shaped GaN nanowires on gold (Au)-coated n-type Si(1 0 0) substrates by using the VPE method. The resulting nanowires had a single-crystalline hexagonal wurtzite structure without any other phases present. The diameters of the nanowires were successfully controlled by changing the main growth time. The morphological, structural, and FE characteristics of the GaN nanowires were investigated.

2. Experimental details

GaN nanowires were synthesized in a horizontal quartz-tube hot-wall VPE system, as depicted in Fig. 1. The system consists of three heater zones, whose temperatures can be controlled individually. The Si(1 0 0) substrates were sequentially cleaned in trichloroethylene, acetone, and ethanol solutions, using an

* Corresponding author at: SKKU Advanced Institute of Nanotechnology (SAINT), Sungkyunkwan University, Suwon 440-746, Republic of Korea.
Fax: +82 31 290 7371.
E-mail address: dhyoon@skku.edu (D.H. Yoon).

0022-0248/$ - see front matter © 2008 Elsevier B.V. All rights reserved.
doi:10.1016/j.jcrysgro.2008.09.033

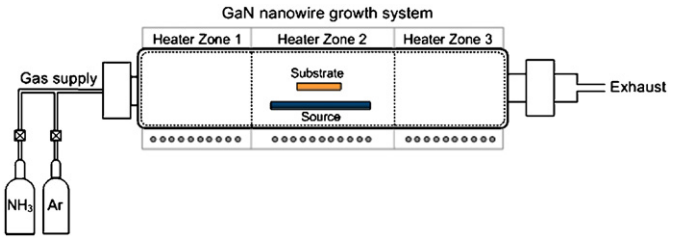

Fig. 1. Schematic representation of the reactor for the growth of the GaN nanowires using the VPE method.

ultrasonic cleaner. Au thin films with layer thicknesses of 3 nm were deposited onto the Si substrates by a thermal evaporation system equipped with a quartz crystal thickness monitor to obtain the precise Au film thickness. The starting materials (source) were high-purity GaN powders (Aldrich, 99.999%) and molten Ga metal (Aldrich, 99.9999%), mixed with a 1:1 weight ratio. The source was put into an alumina boat. The Si substrates ($1 \times 1\,cm^2$) were placed 1 cm from the source. Next, the alumina boat was transferred to the central heater zone inside the reaction chamber. After evacuating to a pressure of $\sim 10^{-3}$ Torr (to remove residual gas), the chamber was heated and filled with ultra-high-purity Ar (99.999%) gas at the flow rate of 1000 sccm. The pressure was kept at 200 Torr during the entire procedure. Additionally, for the main growth period (at a temperature of 950 °C), high-purity NH_3 (99.99%) gas, with flow rate of 20 sccm, was introduced into the system. The main growth time was varied between 15 and 30 min.

The shape and morphology of the GaN nanowires were characterized using FE scanning electron microscopy (FESEM, Jeol 7401). The crystallinity of the GaN nanowires was analyzed using X-ray diffraction (XRD, Bruker AXS D8 Discover) with CuK radiation ($\lambda = 0.1542$ nm). The microstructures were characterized using transmission electron microscopy (TEM, Jeol JEM-3010) and micro-Raman measurements. An Ar laser (514.5 nm, 1 mW) was used as the light excitation source in the micro-Raman spectroscopy. The electrical characteristics were measured using a Keithley 237 source measurement unit. The emission characteristics of the samples were measured in a high-vacuum chamber at a pressure of $\sim 5 \times 10^{-6}$ Torr at RT, with the inter-electrode distance kept at $\sim 200\,\mu m$.

3. Results and discussion

As-grown GaN nanowires on Au-thin-film-coated Si(1 0 0) substrates were produced using the VPE method. As shown in Fig. 2, the rather straight nanowires were distributed on the entire Si substrate surface. The nanowires, with diameters in the range of 20–60 nm and lengths of several micrometers, possessed triangular-shaped cross-sections. Interestingly, from the high-magnification FESEM image of several triangular-shaped GaN nanowires (in Fig. 2(b)), it can be seen that the GaN nanowires have sharp ends and rough surfaces. From the inset of Fig. 2(a), it can be seen that there are Au catalysts at the ends of the nanowires, indicating that the growth mechanism of the GaN nanowires in this study is based on a vapor–liquid–solid (VLS) mechanism [15]. For further structural information on the GaN nanowires, TEM and high-resolution TEM (HRTEM) analyses were executed. Fig. 3(a) shows a low-magnification TEM image of an individual as-grown GaN nanowire. The individual nanowire possessed a uniform diameter of about 60 nm with a sharp end and a rough surface. Fig. 3(b) shows a HRTEM image of a sharp end with no defects. The inset of Fig. 3(b) is the corresponding fast Fourier transform (FFT) pattern of the single nanowire, which can be indexed to the diffraction of a hexagonal wurtzite GaN crystal

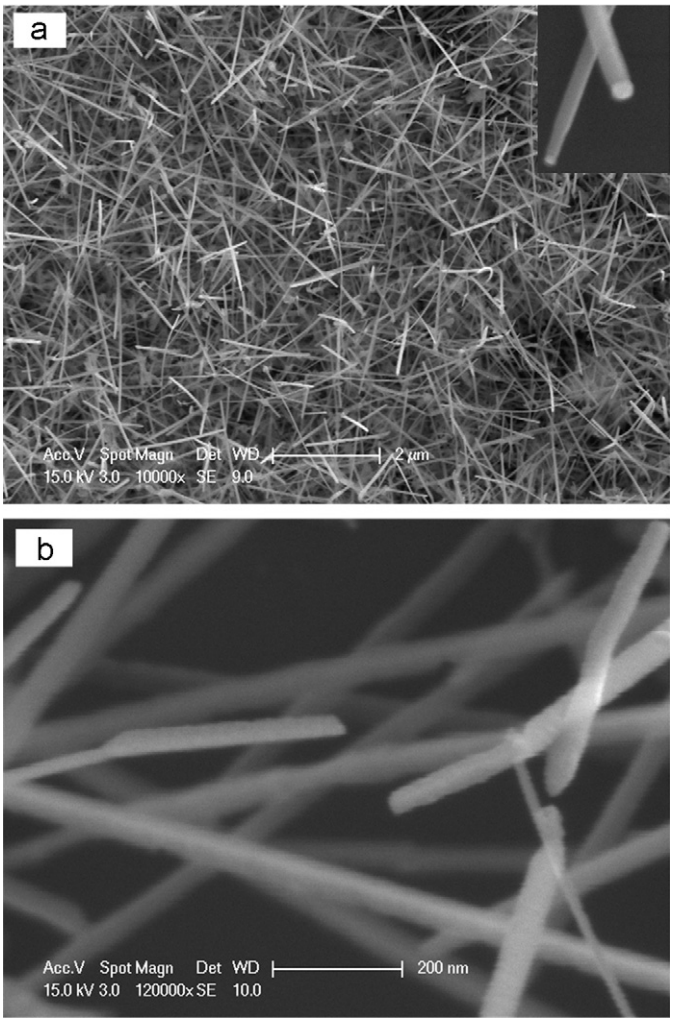

Fig. 2. FESEM images of GaN nanowires on Si(1 0 0) at (a) low magnification and (b) high magnification. The inset shows the existence of the Au catalysts at the end of the nanowires.

along the [1 1 0] direction. Both the HRTEM image and the diffraction pattern indicate the growth of single-crystalline GaN nanowires with high crystallinity.

The growth mechanism of the as-grown GaN nanowires was due to the VLS process with the presence of Au catalysts. Some groups successfully fabricated GaN nanowires by direct reaction of Ga vapor with NH_3 [16] or by sublimation of GaN powder under a flowing NH_3 [17]. However, in our experiment, we could not have GaN nanowires when independently using either Ga liquid or GaN powder. As our purpose, the mixture of Ga/GaN was used as a Ga source. GaN powder also was probably supplied nitrogen (N) by the decomposition process. The reactions can be expressed as

$$Ga_{(l)} \rightarrow Ga_{(g)} \quad (1)$$

$$GaN_{(s)} \rightarrow Ga_{(g)} + N_{(g)} \quad (2)$$

$$2Ga_{(g)} + 2NH_{3(g)} \rightarrow 2GaN_{(s)} + 3H_{2(g)} \quad (3)$$

The presence of H_2 in Eq. (3) caused the growth processes to happen under reduction atmosphere condition.

The XRD measurements were carried out to investigate the crystal structure of the GaN nanowires grown on the Si(1 0 0) substrates. Fig. 4 shows that the peaks at (1 0 0), (0 0 2), (1 0 1), (1 0 2), (1 1 0), and (1 0 3) can be indexed to the peaks of hexagonal wurtzite GaN nanowires with lattice constants of $a = 0.318$ nm

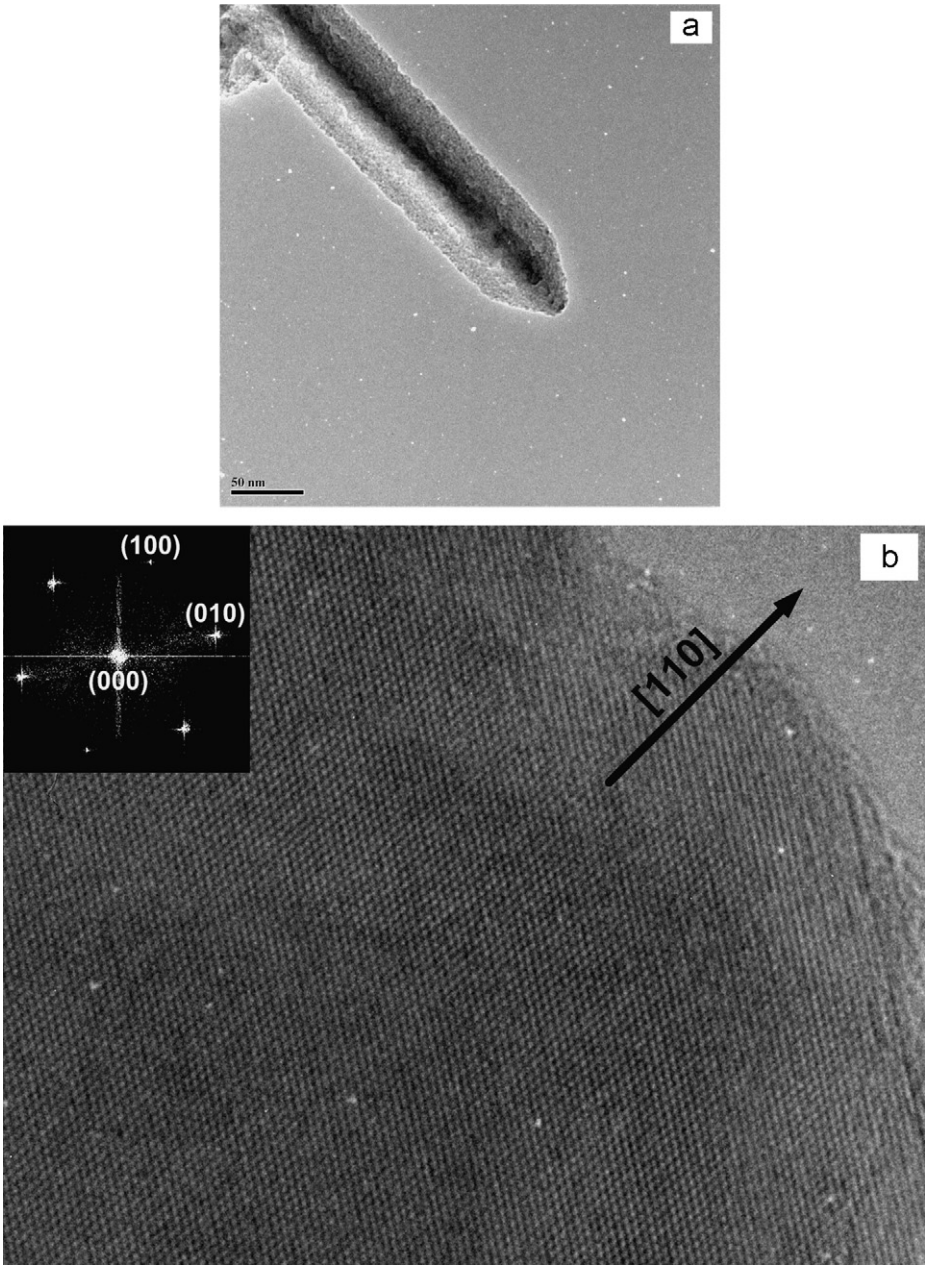

Fig. 3. (a) Low magnification and (b) HRTEM along with corresponding FFT pattern images of the individual GaN nanowire.

and $c = 0.518$ nm. These values are in good agreement with those listed in the JCPDS card for wurtzite GaN (card number 50–0792). No cubic phase of GaN was found. The reflection peak at $2\theta = 61.64$ (noted by K_β) corresponds to the Si(4 0 0)–CuK_β reflection, which is from the single-crystalline Si substrate. The GaN-related diffraction peaks are slightly shifted to higher diffraction angle (e.g. $\Delta(2\theta) = 0.14$, 0.017, and 0.047 for (1 0 0), (0 0 2), and (1 0 1) peaks, respectively). Due to the different properties between GaN and Si substrate such as lattice mismatch and thermal conductivity, this causes the random orientation and biaxial compressive stresses in the inward radial direction of the GaN nanowires [18].

Fig. 5 shows the backscattering Raman spectrum (over a wavenumber range of 250–800 cm^{-1}) of the GaN nanowires on the Si(1 0 0) substrate at RT. The GaN phonon modes are A_1+E_1+2B_1+2E_2, where the A_1(LO), E_1(TO), E_2(high), and (low) modes are Raman-active, and the two B_1(silent) modes are Raman-inactive. The peaks at 556.5, 567.5, and 728.5 cm^{-1} may be the E_1(TO), E_2(high), and A_1(LO) modes, respectively (labeled in Fig. 5). The sharp, strong E_2(high) phonon peak in the Raman spectrum at 567.5 cm^{-1} confirms that the phase of the GaN nanowires is wurtzite. This is in good agreement with the XRD result. The low-intensity ratio of $I(E_2(\text{high})/I(A_1(\text{LO}))$ indicates high crystallinity of the GaN nanowires. Nevertheless, Raman scattering is strongly sensitive to surface states and nanosize effects, causing a low-energy shift of 1.5 cm^{-1} of E_2(high) compared to the theoretical value of 569 cm^{-1} [19]. This low-energy shift of E_2(high) might be attributed to the biaxial compressive stresses within the GaN nanowires, as discussed in XRD result [18]. Moreover, the peaks at 303, 520, and 672 cm^{-1} are derived from the Si substrate. One additional peak is also found at 420 cm^{-1}, which is not permitted by the C_{6v}^4 space group in the first-order Raman scattering at the zone center. It might be attributed to the acoustic overtone region with (A_1+E_2) symmetry

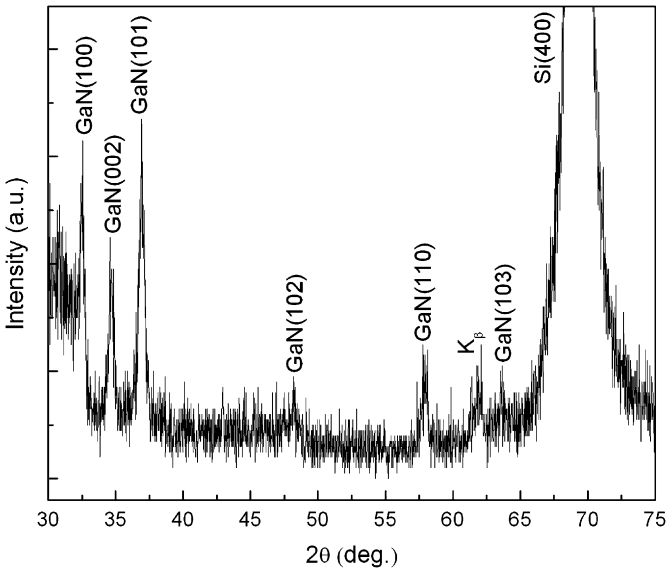

Fig. 4. XRD spectrum of the GaN nanowires grown on the Si(1 0 0) substrate.

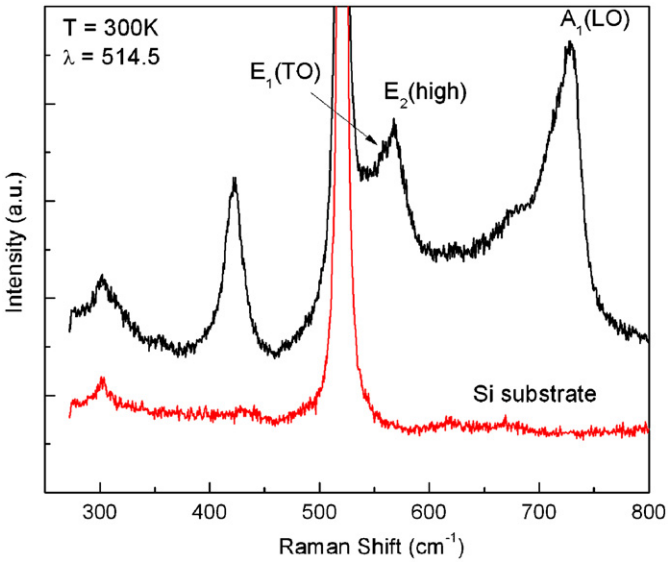

Fig. 5. Raman spectrum of the GaN nanowires. The red spectrum is that of the Si substrate.

derived from the second-order Raman scattering [20–22]. No Raman peaks relating to cubic GaN were observed, such as the TO and LO phonon modes of a cubic GaN lattice at 553 and 739 cm^{-1}, respectively.

The relationship between the current (I) and voltage (V) of the electron FE from the as-grown GaN nanowires was theoretically evaluated using the simplified Fowler–Nordheim (FN) equation $I = (A\beta^2V^2/\varphi)\exp(-B\varphi^{3/2}/\beta V)$ [23,24], where I (A/cm^2) is the electron current density of the sample, A and B are constants with values of 1.56×10^{-10} (AV^{-2} eV) and 6.83×10^{3} ($VeV^{-3/2}$ μm^{-1}), respectively, V (V) is the applied voltage, φ (eV) is the work function of the emitter, and β is a field enhancement factor that depends on the geometry of the emitter (e.g. the shape and diameter).

The FE measurements were collected within a vacuum chamber at a low pressure of $\sim5\times10^{-6}$ Torr. A direct current

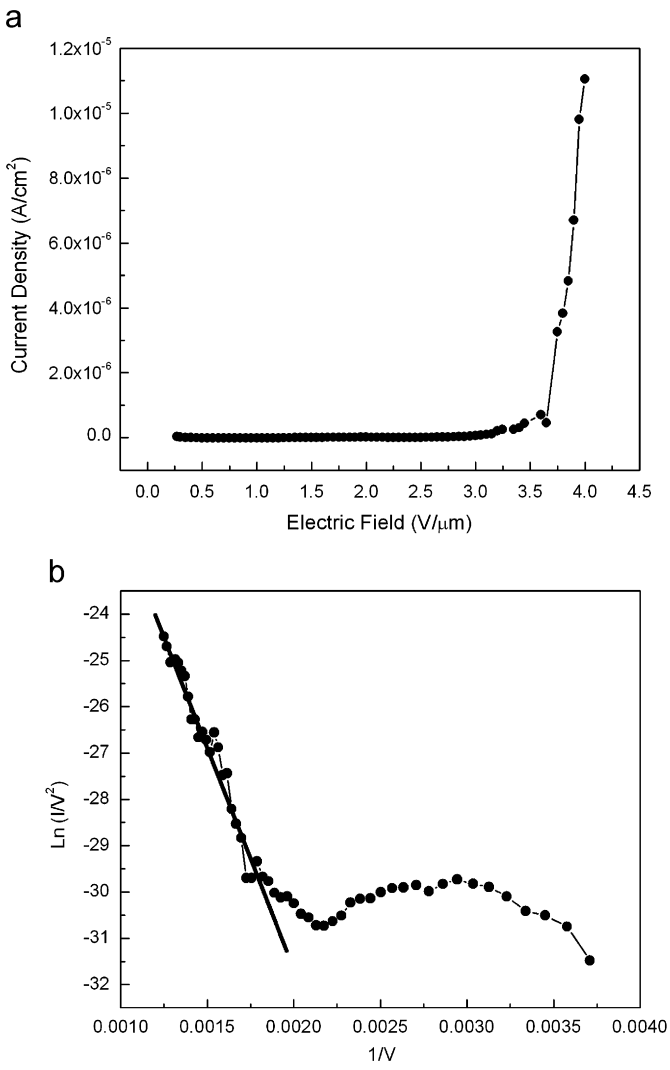

Fig. 6. (a) FE curve of the GaN nanowires on the Si substrate and (b) Fowler–Nordheim plot.

voltage increasing from 0 to 1000 (V) was applied to the GaN nanowires, which was the cathode. An indium tin oxide (ITO)-coated glass was used as the anode. The emission area was about 1×1 cm^2 and the inter-electrode distance was maintained at ~200 μm. Fig. 6(a) and (b) shows the FE measurements and a corresponding FN plot of the as-grown GaN nanowires on the Si substrate, respectively. The turn-on electric field was defined as the electric field required to obtain a current density of 10 μA/cm^2. As observed in Fig. 6(a), the turn-on field was estimated to be ~3.96 V/μm, which is lower than that quoted in previous reports (e.g. 6.1 V/μm from GaN nanobelts [9] and 7.0–9.5 V/μm from GaN nanowires [10–14]). The straight line in Fig. 6(b) indicates FN tunneling behavior of the semiconducting GaN nanowires; thus, the electron emission is indeed caused by vacuum tunneling. The field enhancement factor can be calculated from the slope (k_{FN}) of the $(1/V)$–$\ln(I/V^2)$ curve, using this equation $\beta = -(B\times d_{A\_C}/k_{FN})\varphi^{3/2}$, where d_{A_C} is the inter-electrode distance. With the GaN work function of 4.1 eV and $d_{A\_C} = 200$ μm, the value of β is estimated to be ~1050, which is acceptable for the applications of FE displays. The current β value of 1050 is higher than those previously reported for GaN nanowires [12,14]. The reason for this can be attributed to the sharp ends and rough surfaces of the GaN nanowires.

4. Conclusion

The hexagonal wurtzite GaN nanowires with triangular-shaped cross-sections, grown on Si (1 0 0) substrates, were produced via a process based on the VPE method, using a mixture of molten Ga and GaN powders with a constant flowing rate of NH_3 gas. The structural properties of the GaN nanowires were investigated by TEM and micro-Raman spectroscopy. The Raman modes were observed at 420, 556.5, 567.5, and 720 cm^{-1}; the low-intensity ratio between E_2(high) and A_1(LO) is due to the high crystallinity of the GaN nanowires. In the FE measurements (at RT), we obtained a turn-on field as low as ~3.96 V/μm and a field enhancement factor of ~1050.

Acknowledgements

The authors thank J. H. Park for his assistance with the use of the FE tool. Author Dinh thanks the SKKU Advanced Institute of Nanotechnology (SAINT) of Korea for supporting his graduate study with a research scholarship.

References

[1] Y. Huang, X.F. Duan, Y. Cui, C.M. Lieber, Nano Lett. 2 (2002) 101.
[2] H.J. Dai, A. Javey, E. Pop, D. Mann, Y.R. Lu, NANO: Brief Rep. Rev. 1 (2006) 1.
[3] K. Nikolic, M. Forshaw, R. Companó, Int. J. Nanosci. 2 (2003) 7.
[4] Y.B. Li, Y. Bando, D. Golberg, K. Kurashima, Appl. Phys. Lett. 81 (2002) 5048.
[5] J.P. Sun, Z.X. Zhang, S.M. Hou, G.M. Zhang, X.Y. Zhao, W.M. Liu, Z.Q. Xue, Appl. Phys. A 75 (2002) 479.
[6] C.J. Lee, T.J. Lee, S.C. Lyu, Y. Zhang, H. Ruh, H.J. Lee, Appl. Phys. Lett. 81 (2002) 3648.
[7] R.J. Nemanich, M.C. Benjamin, S.P. Bozeman, M.D. Bremser, S.W. King, B.L. Ward, R.F. Davis, B. Chen, Z. Zhang, J. Bernhole, Mater. Res. Soc. Symp. Proc. 77 (1996) 395.
[8] S. Nakamura, T. Mukai, M. Senoh, Appl. Phys. Lett. 64 (1994) 1687.
[9] L. Luo, K. Yu, Z. Zhu, Y. Zhang, H. Ma, C. Xue, Y. Yang, S. Chen, Mater. Lett. 58 (2004) 2893.
[10] X. Xiang, H. Zhu, Appl. Phys. A 87 (2007) 651.
[11] B.D. Liu, Y. Bando, C.C. Tang, F.F. Xu, J.Q. Hu, D. Golberg, J. Phys. Chem. 109 (2005) 17082.
[12] T.Y. Kim, S.H. Lee, Y.H. Mo, H.W. Shim, K.S. Nahm, E.-K. Suh, J.W. Yang, K.Y. Lim, G.S. Park, J. Crystal Growth 257 (2003) 97.
[13] B.D. Liu, Y. Bando, C. Tang, F. Xu, D. Golberg, Appl. Phys. Lett. 87 (2005) 73106.
[14] D.K.T. Ng, M.H. Hong, L.S. Tan, Y.W. Zhu, C.H. Sow, Nanotechnology 18 (2007) 375707.
[15] R.S. Wagner, W.C. Ellis, Appl. Phys. Lett. 4 (1964) 89.
[16] J. Zhang, X.S. Peng, X.F. Wang, Y.W. Wang, L.D. Zhang, Chem. Phys. Lett. 345 (2001) 372.
[17] X.F. Duan, C.M. Lieber, J. Am. Chem. Soc. 122 (2000) 188.
[18] H.W. Seo, S.Y. Bae, J.H. Park, H. Yang, K.S. Park, S.S. Kim, J. Chem. Phys. 116 (2002) 9492.
[19] T. Ogino, M. Aoki, Jpn. J. Appl. Phys. 19 (1980) 2395.
[20] H. Siegle, G. Kaczmarczyk, L. Fillipidis, A.P. Litvinchuk, A. Hoffmann, C. Thomsen, Phys. Rev. B 55 (1997) 7000.
[21] H.L. Liu, C.C. Chen, C.T. Chia, C.C. Yeh, C.H. Chen, M.Y. Yu, S. Keller, S.P. DenBaars, Chem. Phys. Lett. 345 (2001) 245.
[22] W. Limmer, W. Ritter, R. Sauer, B. Mensching, C. Liu, B. Rauschenbach, Appl. Phys. Lett. 72 (1998) 20.
[23] R.H. Fowler, L. Nordheim, Proc. R. Soc. London Ser. A 119 (1928) 173.
[24] Nordheim, Proc. R. Soc. London Ser. A 121 (1928) 626.